Benthic Storms, Vortices, and Particle Dispersion in the Deep West European Basin

Holger Klein

UDC 551.465.58:551.465.15: North Atlantic

Summary

During the NOAMP Experiment (September '83 to May '86), 20 benthic storms with velocities of up to 27 cm/s and a duration of between 3 and 25 days, have been observed in a region centered at 47° 20′ N and 20° W. The calculation of streamfunction maps shows clearly, that all storms between September '83 and September '84 occur in connection with deep reaching synoptic vortices. These events are important mechanisms for the dispersion of tracers, which are released at the seabed. They enable the particles to pass the interface between the well-mixed bottom boundary layer and the stratified interior of the deep sea. The eddies, with lifetimes of up to several months, trap the particles and facilitate horizontal and vertical transports within the eddy. Each vortex, by means of its shear, deforms a parcel of contaminated water to thin sheets, respectively to thin filaments with regard to two dimensions. This makes small-scale mixing processes work effectively.

Tiefseestürme, Wirbel und Teilchenausbreitung in der Tiefsee des Westeuropäischen Beckens (Zusammenfassung)

Während des NOAMP-Experiments wurden in einem Gebietbei 47° 20′ N und 20° W 20 Tiefseestürme mit Geschwindigkeiten bis zu 27 cm/s und einer Dauer zwischen 3 und 25 Tagen gemessen. Stromfunktionskarten zeigen, daß, zumindest im Zeitraum von September '83 bis September '84, die Stürme stets im Zusammenhang mit tiefreichenden synoptischen Wirbeln auftreten. Diese Ereignisse sind von herausragender Bedeutung für die Ausbreitung am Tiefseeboden eingebrachter Stoffe. Sie ermöglichen den Austausch von Wasserkörpern durch die Sprungschicht zwischen der stark durchmischten Bodengrenzschicht und dem geschichteten Inneren der Tiefsee. Die Wirbel, mit Lebenszeiten bis zu mehreren Monaten, können Wasserkörper mit Eigenschaften, die ihn von der umgebenden Wassermasse unterscheiden, einfangen und transportieren sie vertikal und horizontal innerhalb des Wirbels. Jeder Wirbel deformiert solche Wasserkörper zu dünnen Scheiben, bzw. zu dünnen Filamenten im Zweidimensionalen, und schafft somit die notwendige Voraussetzung für das Wirken kleinskaliger Vermischungsprozesse.

Tempêtes de grands fonds, tourbillons, dispersion de particules dans les eaux profondes du Bassin de l'Europe de l'Ouest (Résumé)

Durant l'expérience NOAMP (septembre 1983 – Mai 1986), vingt tempêtes de grands fonds avec des vitesses supérieures à 27 cm/s et des durées comprises entre 3 et 25 jours, ont été observées dans un secteur centré sur le point 47° 20′ nord et 20° ouest. Le calcul des cartes de courant montre clairement que les tempêtes

sous-marines observées entre septembre 1983 et semtembre 1984 sont reliées à des tourbillons synoptiques atteignant de grandes profondeurs. Ces évènements sont des mécanismes importants pour la dispersion d'éléments – traces libérés sur le fond de l'océan. Ils permettent aux particules de franchir l'interface entre la couche limite de fond, homogène, et la partie stratifiée de la mer profonde. Les tourbillons qui ont des durées de vie de plusieurs mois, piègent les particules et facilitent leurs transports horizontaux et verticaux au sein même du tourbillon. Chaque tourbillon du fait du cisaillement, transforme un volume d'eau contaminée en minces couches, ou plutôt en minces filets d'eau, si l'on se place dans les deux dimensions. Cela génère en réalité un processus de mélange à petite échelle.

Introduction

The NOAMP Experiment (Nordostatlantisches Monitoring-Programm), carried out from September '83 until May '86, was designed to investigate the local transport in the deep North East Atlantic, also with regard to the fate of matter released at the seabed. During the experiment, 7 current meter moorings were located in an area between 47° 10′ N and 47° 35′ N and 18° 45′ W and 20° 35′ W. All moorings had current meters with a nominal distance from the bottom of 10, 30, 70, 200, and 250 metres. Most of the deepest instruments, i. e. 10 m above the bottom (hereafter a. b.), were acoustical Neil-Brown instruments, the others were Aanderaa ACM5 current meters.

The mean velocity near the bottom, i. e. less than 75 m a. b., range from about 2 to 6 cm/s (Mittelstaedt, Bock, Bork, et al. [1986]). These values agree well with the results of other experiments in the deep North East Atlantic (Dickson, Gould, Müller et al. [1985], Vangriesheim [1986]).

Approaching towards the bottom, mean (K_m) and eddy kinetic energy (K_e) increases, showing a local maximum between 10 and 100 m a. b. (see Fig. 2). This is the dynamic signal of the bottom boundary layer (hereafter BBL), which is also characterized by homogeneity of potential temperature, salinity, and other properties, and a strong increase of the concentration of suspended matter due to bottom friction (see also Fig. 11). In the NOAMP area, the height of the BBL ranges between 20 and 150 metres, depending upon the velocity present. Matter, released at the seabed, is expected to be mixed within the BBL within several hours or a few days. At the top of the BBL a front is usually given by a pycnocline which reduces the exchange with the interior of the deep ocean significantly (Robinson and Kupferman [1985]).

During the whole experiment, episodic events with unusually high velocities, known in the literature as benthic, abyssal or deep-sea storms, can be read from the deepest current meters (less than 70 m a. b.). In the NOAMP experiment, a benthic storm is defined as a period for at least 48 hours with velocities of more than 10 cm/s.

During NOAMP storms with a duration of between 3 and 25 days and velocities of more than 25 cm/s have been measured at different moorings (see Table 1). The positions of the moorings are marked in Fig. 1.

Fig. 1. The NOAMP area with moorings, at which benthic storms have been observed. Dotted line: Area, in which the streamfunction has been calculated

Table 1
Benthic storms during NOAMP

Date	Mooring	Duration d	
16. 11. 83–18. 11. 83	L1	3	A
22. 11. 83– 3. 12. 83	K2	12	B
11. 6. 84–18. 6. 84	L1	8	C
20. 7. 84–24. 7. 84	K2	5	D
15. 11. 84–23. 11. 84	K9	9	
21. 11. 84–25. 11. 84	K1	4	
28. 11. 84– 3. 12. 84	K1	6	
19. 4. 85–24. 4. 85	K1	6	
1. 5. 85– 8. 5. 85	K1	8	
1. 9. 85– 7. 9. 85	K1	7	
10. 9. 85–15. 9. 85	K13	6	
24. 11. 85–30. 11. 85	D2	7	
28. 11. 85–17. 12. 85	K10	20	
3. 5. 86–27. 5. 86	K10	25	
15. 5. 86–27. 5. 86	K12	13	
23. 9. 85–27. 9. 85	K13	5	
7. 10. 85–12. 10. 85	K13	6	
20. 11. 85–25. 11. 85	K13	6	
4. 2. 86–24. 2. 86	K13	21	
21. 5. 86–25. 5. 86	K13	5	

A, B, C, and D label the storms, which occurred during NOAMP I and II

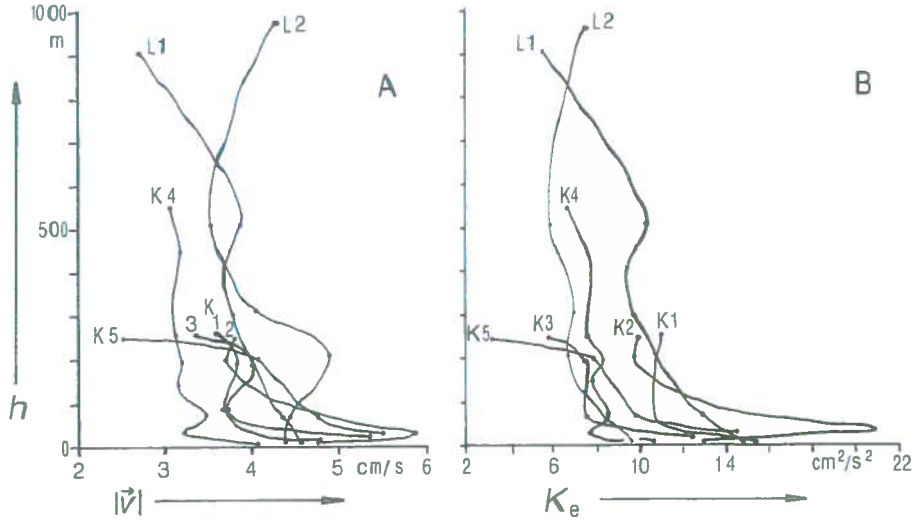

Fig. 2. Amount of velocity $|\vec{v}|$ (A) and eddy kinetic energy K_e (B) versus distance from bottom h

The storms occur both at moorings near topographic features and in areas with only modest slopes. Similar events have been reported by Hollister and McCave [1984] from a region under the Gulf Stream. They supposed that the origin of high abyssal kinetic energy is related to high surface kinetic energy, i. e. the Gulf Stream or its rings. In the NOAMP area, the benthic storms are probably due the synoptic eddies: as for example surveyed during "Meteor" 70 cruise (Kupferman, Becker, Simmons et al. [1986]. Mittelstaedt [1987]). Such storms, especially in connection with deep reaching vortices, are important mechanisms for the dispersion of particles: they enhance the height of the BBL and the amount of K_m and K_ϱ, and enable the particles to pass the interface between BBL and the interior of the deep ocean.

Divergences caused by deep reaching eddies or topographic features maintain the exchange between both layers (eddy or topographic pumping). Fig. 3 shows a part of the low-pass filtered time series of mooring K2 (10 m a. b.), with storm B of Table 1. The original data exceed 20 cm/s during the storm. The mean value of the whole 6 month record is 4.8 cm/s.

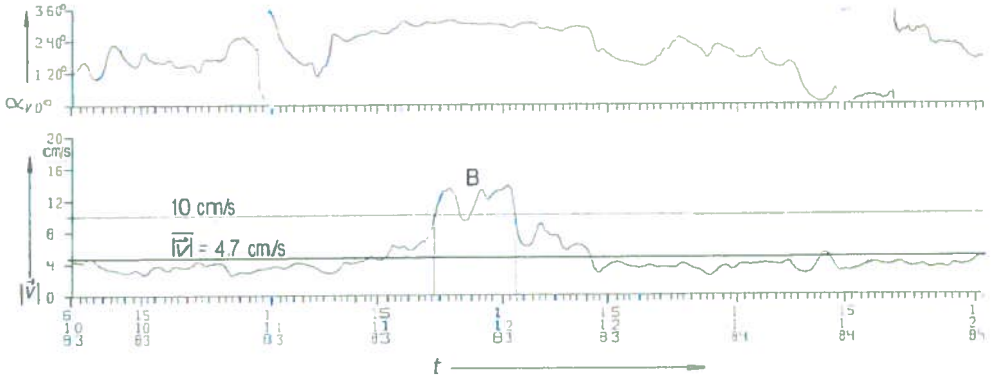

Fig. 3. Time series of amount of velocity $|\vec{v}|$ and direction α, of mooring K2, 10 m a. b., with storm B

Benthic storms and deep reaching vortices during NOAMP I and II

From September '83 until April '84 (NOAMP I), all moorings – with the exception of mooring K5 – were located in the abyssal plain westwards of the major topographic feature, the "Großer Dreizack" (Heinrich [1986]). In the long-term mean, there is a strong westward flow in the northern part of the plain (at L2, K3, L1) and a weak counter current in the south at K1, probably induced by the topography. At 10 m and 70 m a. b. the instruments yield good data for 5 current meters, in 200 m a. b. for 6 current meters (see Table 2).

Table 2

distance from bottom	moorings with good data
m	
10	K1, K2, K4, L1, L2
70	K1, K3, K4, L1, L2
200	K1, K2, K3, K4, L1, L2

Five current meters, with 2 velocity components each, supply a total of 10 informations. Therefore, a streamfunction ψ can be approximated by a cubic polynomia

$$\psi = \sum_{\nu+\mu=1}^{3} a_{\nu\mu} x^{\nu} y^{\mu}$$

with x and y the coordinates of the current meters. With positions related to the centre of the gravity system

$$\bar{x} = \frac{1}{n}\sum_{i=1}^{n} x_i := 0 \quad \text{and} \quad \bar{y} = \frac{1}{n}\sum_{i=1}^{n} y_i := 0$$

and n the number of current meters, the equation reads shorter. The coefficients $a_{\nu\mu}$ are fitted to the measurements by the method of least square sums, i. e.

$$\sum_{i=1}^{n} ((\psi_{x_i} - v_i)^2 + (\psi_{x_i} + u_i)^2) = \text{minimum}(a_{\nu\mu}),$$

and with u and v the velocity components in east-west and north-south direction respectively. The introduction of a horizontal streamfunction ψ, respectively the neglect of the vertical velocity component, is reasonable because the latter is about 2 to 3 orders of magnitude smaller than the horizontal velocity, i. e. in the order of magnitude of 1 m/d.

To reconstruct the synoptic-scale flow pattern, the coefficients $a_{\nu\mu}$ have been determined from vector averaged daily mean values. The polygon spread out by the current meters has a maximum extension in west-east direction of 48 km, and 30 km in north-south direction (see dotted line in Fig. 1). The Rossby deformation radius, giving the horizontal scale for synoptic eddies, i. e. periods from days to months and scales of tens or some hundreds of kilometres (Kamenkovich, Koshlyakov and Monin [1986])

$$L_R = \frac{\bar{N}}{f} H$$

amounts about 70 km in the NOAMP area (Coriolis parameter $f = 1.075 \times 10^{-4}$ 1/s, depth of the ocean $H = 4500$ m and depth-averaged Brunt-Väisälä frequency $\bar{N} = 2.8 \times 10^{-4}$ 1/s).

It is obvious that the streamfunction maps – reliable only inside the current meter polygon – cannot picture a synoptic vortex as a whole. The storms occurring during NOAMP I are labelled with A and B in Table 1. Figures 4 and 5 show streamfunction maps for both storms at 10, 70 and 200 m a. b. The vortex structure is evident at all levels. The stars mark the position of the moorings which measured the storm. In both cases, they are located in outer part of the vortex where the highest velocities are expected.

The deepest part of the BBL is the turbulent Ekman layer. Its height h_e can be estimated as

$$h_e = 0.4 \times (u_*/f)$$

with friction velocity $u_* = (1/30)U$ and U the geostrophic velocity outside the BBL (Armi and Millard [1976]).

Table 3

U	h_e
cm/s	m
2.0	2.5
5.0	6.2
10.0	12.4
15.0	18.6
20.0	24.8

The estimate (see Table 3) shows that the storms occur also within, or at least at the top of the turbulent Ekman layer. A vertical shift in the core position between 10 and 70 m a. b. is evident in both figures, due to the interface between BBL and the deep sea. Le Groupe Tourbillon [1983] established a similar phenomena in the Tourbillon Eddy at the main pycnocline, about 5° eastwards of the NOAMP area.

Figure 4 (17. 11. 83) shows a anticyclonic vortex in the northeastern part of the polygon and a small part of a cyclonic vortex in the southwest. The latter moves slowly (1.0 to 1.5 cm/s) northeastwards and shapes the circulation pattern 8 days later on November 25 (see Fig. 5). Its mean rotation period is about 9 days at 10 m a. b. and 12 days at 200 m a. b.

During NOAMP II, i. e. from April '84 until September '84, two storms occurred, labelled with C and D in Table 1. For this period, the streamfunctions can be computed for a very small polygon (ca. 28 km × 28 km) at 70 m a. b. only. Again, the maps indicate the transit of a vortex.

A deep reaching meddy

The streamfunctions in Fig. 6 show a cyclonic vortex, again with strong bottom intensification. This vortex can be tracked for several days during October '83. Its transit velocity, estimated from the displacement of the core, amounts to about 2 to 6 cm/s. The net movement is westwards, but not straight ahead.

The vortex is also evident in the CTD-data of the "Meteor" 65 cruise, September/October '83. Evaluating the data of the hydrographic survey (81 CTD casts in a 120 n. m. × 120 n. m. rectangle), Schauer [1987] established and described a cyclonic vortex with the hydrographic properties of a meddy. With regard to the geopotential between 1600 and 4000 dbar, the meddy is embedded in a field of other cyclonic and anticyclonic features (see Fig. 7). The dynamic signal is centred at 1600 dbar, but the anomalies of potential temperature and density are visible down to the bottom. Using also the current meter data of the French TOPOGULF-moorings, Schauer estimated the transit velocity of the meddy as being between 1.2 and 5.8 cm/s. The geostrophic velocity in the meddy at 1600 m depth is greater than 10 cm/s.

Dispersion of virtual particles

The sampling interval of the current meters is 60 minutes for the ACM5's, respectively 30 minutes for the Neil-Brown instruments. Therefore, the coefficients $a_{\nu\mu}$ of streamfunction ψ can be determined for every full hour. Due to the fitting of the coefficients to direct measurements, the resulting streamfunction pattern includes the effect of momentum flux $\overline{u'v'}$. The calculation of a "time series" of the coefficients $a_{\nu\mu}$ facilitates the simulation of the quasi-lagrangian transport of virtual passive particles.

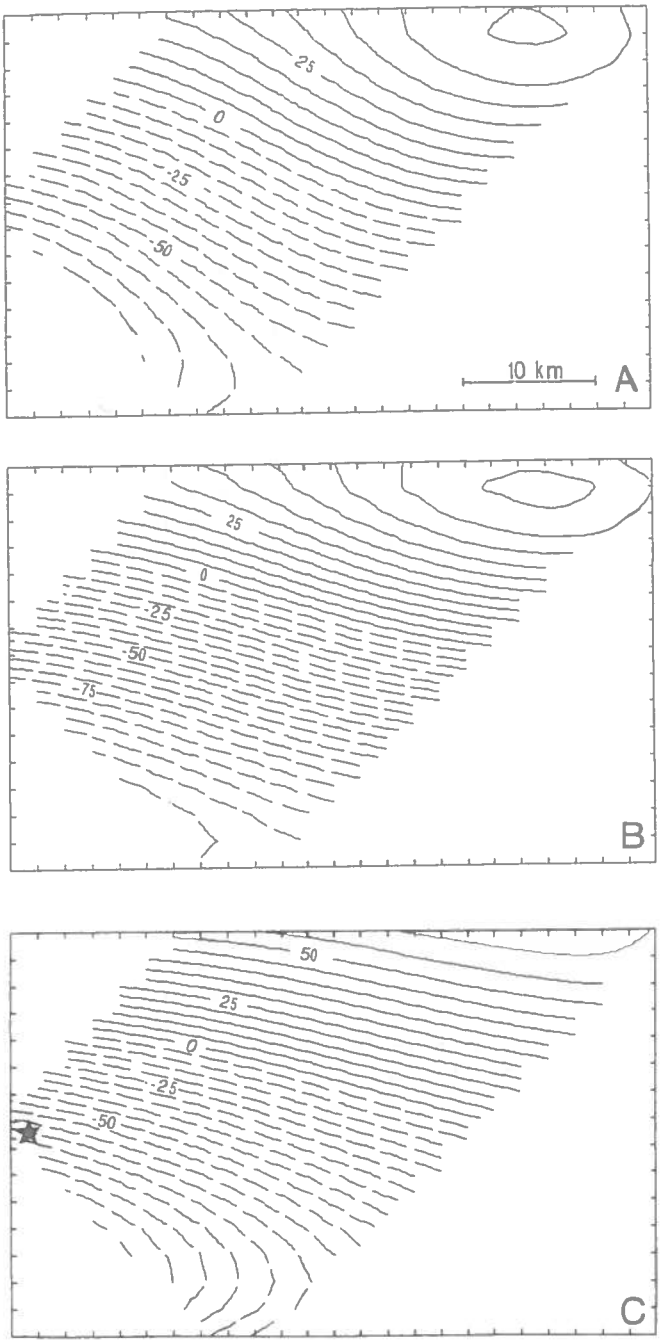

Fig. 4. Streamfunction in cm³/s from daily mean values of November 17 at (A) 200 m, (B) 70 m, and (C) 10 m a. b.
Tick marks represent 2 km, the star the mooring which measured storm A of Table 1

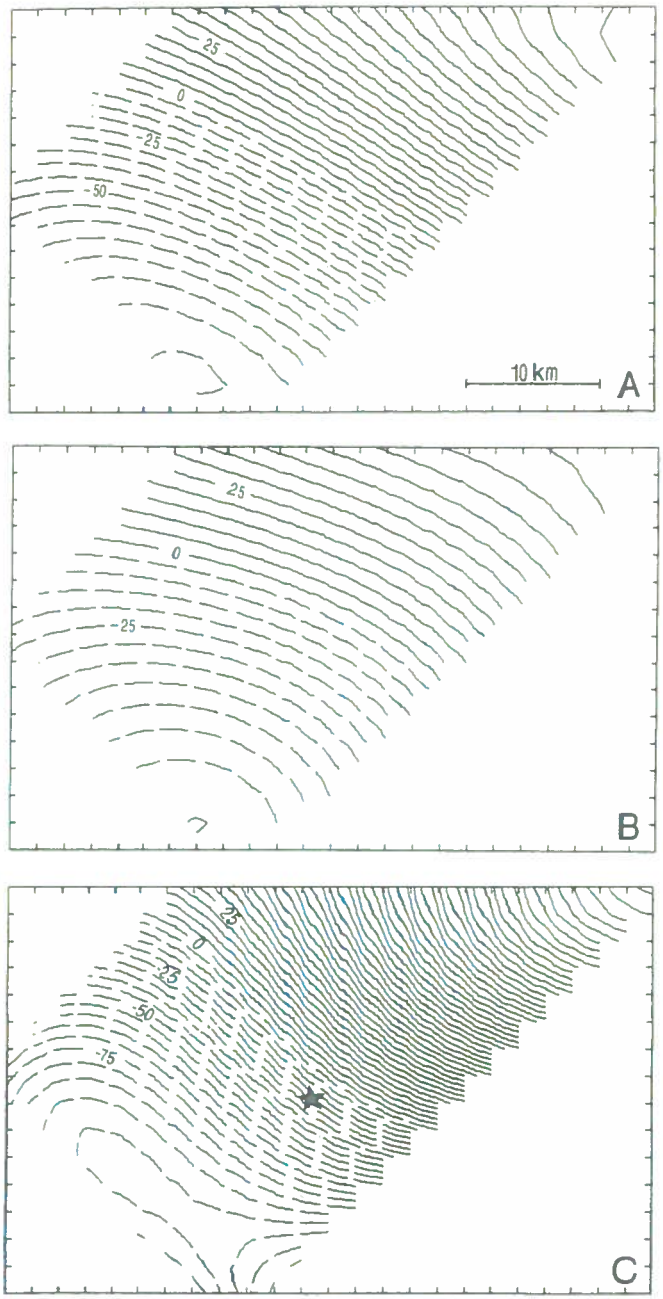

Fig. 5. Streamfunction in cm^2/s from daily mean values of November 25 at (A) 200 m, (B) 70 m, and (C) 10 m a. b.
Tick marks represent 2 km, the star the mooring which measured storm B of Table 1

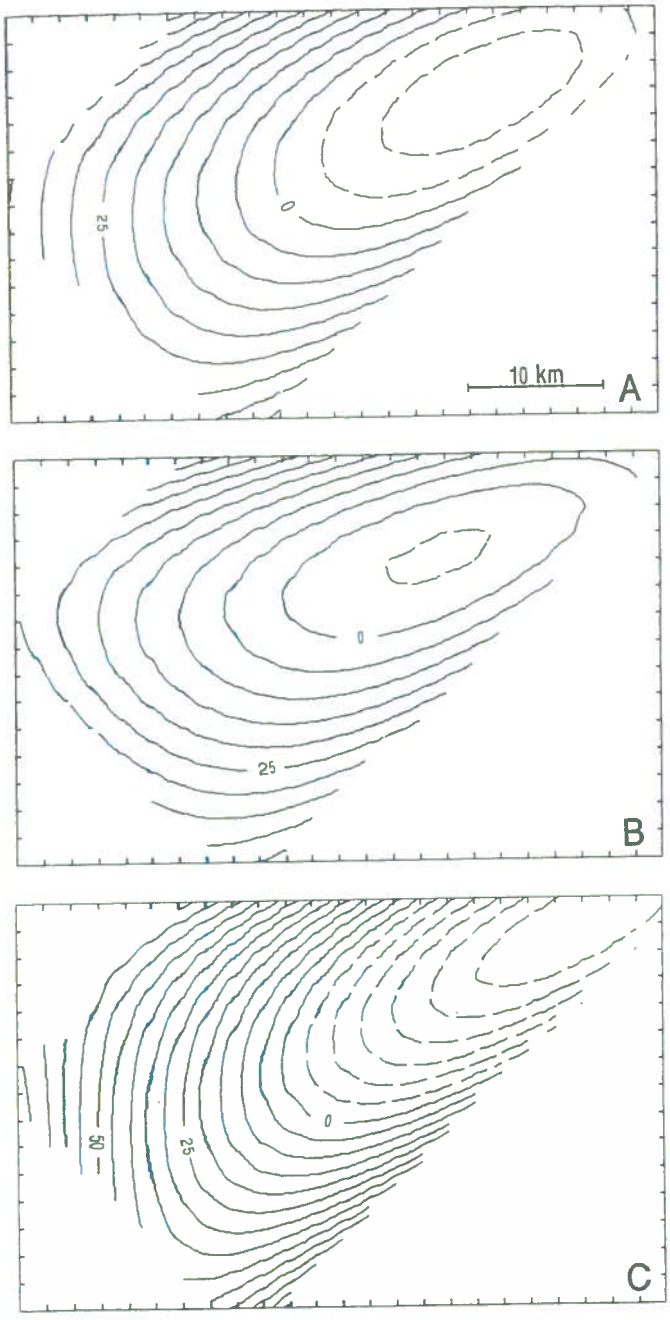

Fig. 6. Streamfunction in cm²/s from daily mean values of October 19 at (A) 200 m, (B) 70 m, and (C) 10 m a. b. (meddy).
Tick marks represent 2 km

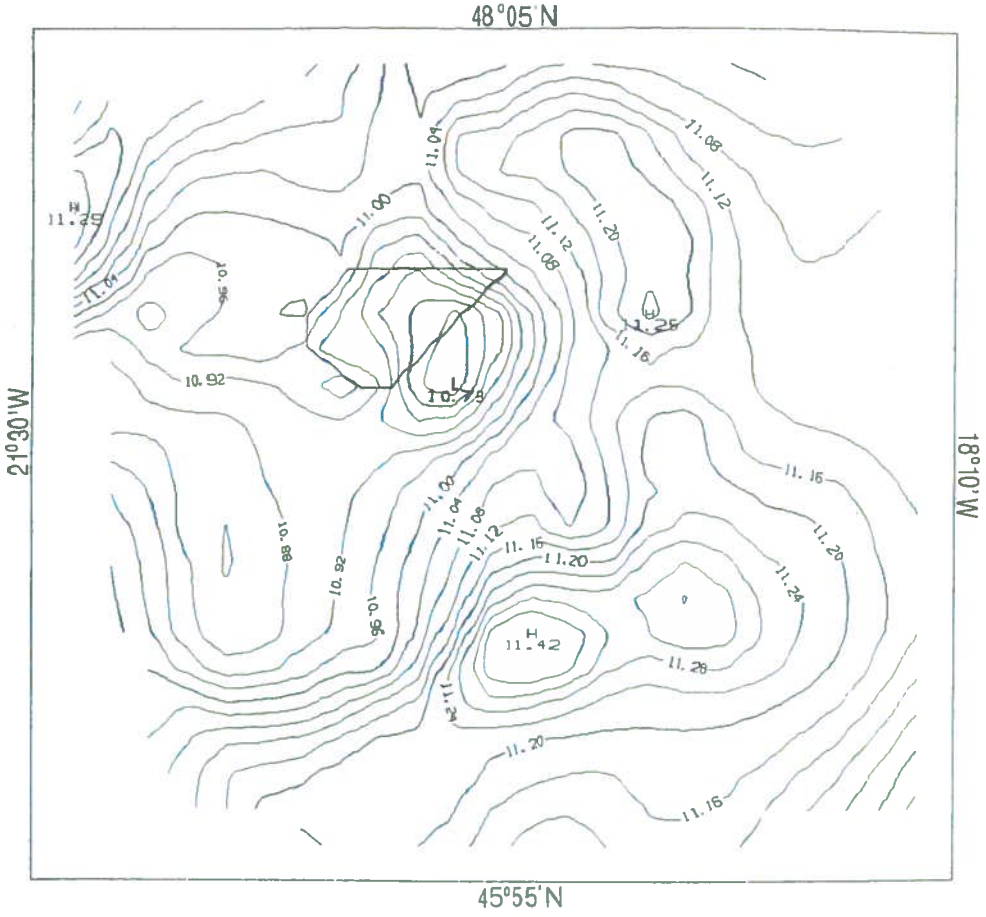

Fig. 7. Geopotential in m^2/s^2 between 1600 and 4000 dbar from Schauer [1987]. The polygon marks the area in which the stream-function has been calculated

The crosses in Fig. 8 and 9 mark the position of a virtual point source: at each time step, i. e. every 60 minutes, one virtual particle is released. Figs. 8 and 9 show the streak lines after 20 days (480 particles released). A streak line is the current location of fluid particles, all of which passed through a fixed point in space (i. e. the source) at some previous time (Streeter [1961]). The Figures are like a picture of a smoke plume leaving a stack: one has no information about the paths of the particles, one sees their final positions only. Particles leaving the polygon are lost, they cannot re-enter it due to the lack of information about the velocity outside the polygon. The numbers of released and lost particles are given in the plots.

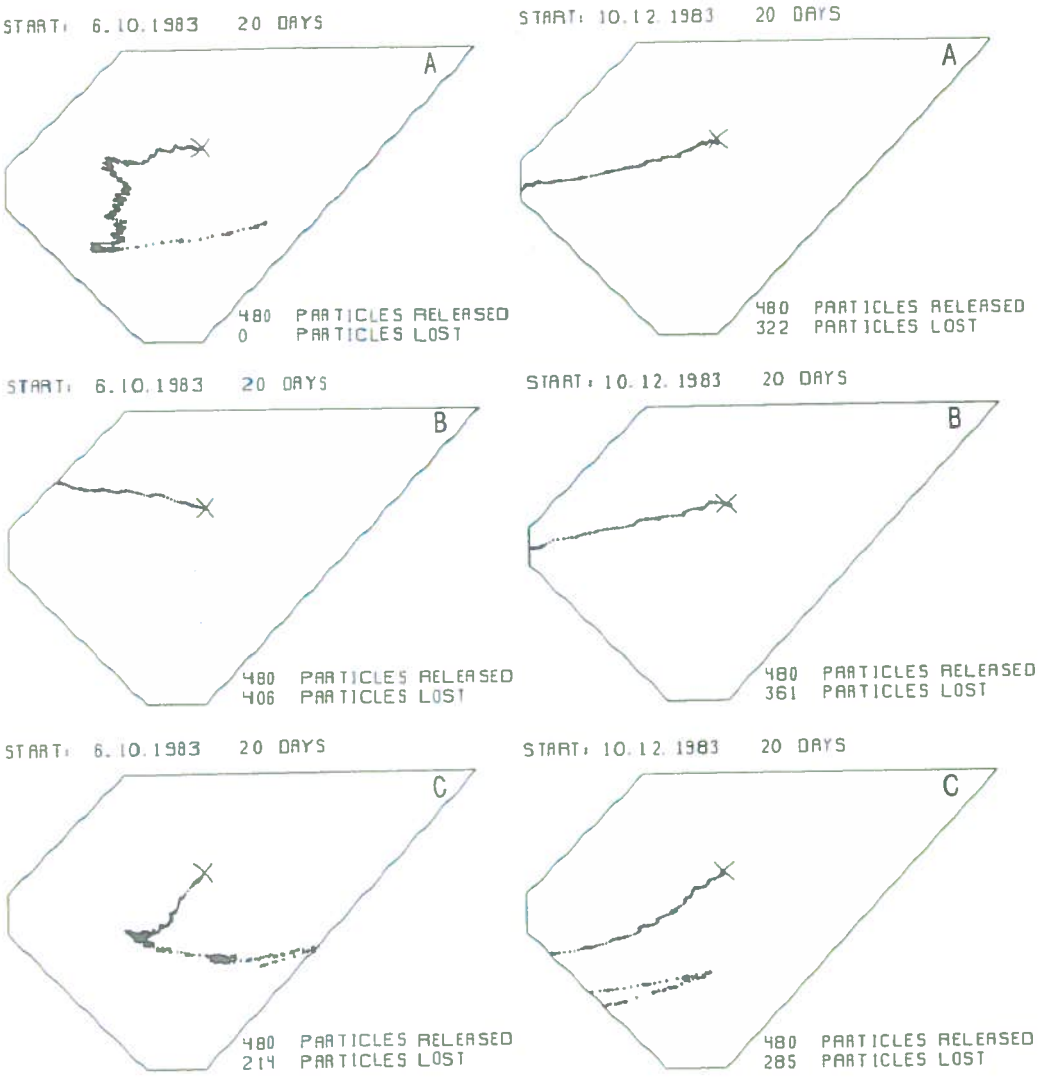

Fig. 8. Simulation of a point source in (A) 200 m, (B) 70 m, and (C) 10 m a. b. The simulation runs from Oct. 6 until Oct. 25

Fig. 9. Simulation of a point source in (A) 200 m, (B) 70 m, and (C) 10 m a. b. The simulation runs from Dec. 10 until Dec. 29

Figure 8 shows the result of a simulation running from October 6 until October 25, i. e. the time the cyclonic meddy passes the polygon. At 200 m a. b. all particles are trapped by the meddy. At 10 m a. b. more than half of the particles released are still inside the meddy. The cyclonic sense of rotation is evident. 70 m a. b. the particles leave the polygon in a westward direction. This may be due either to the curvature of the meddy axis or to the shift of the core position at the pycnocline between BBL and the interior of the deep sea.

The simulation in Fig. 9 begins on December 10. During this time no eddies are observed in the area; the circulation is representative for the mean values about the whole experiment. In each level the particles leave the polygon in a westward direction. Approaching towards the bottom, the flow rotates cyclonically.

Deformation due to shear

Le Groupe Tourbillon demonstrated the deformation of a patch of Mediterranean Water due to shear in the Tourbillon Eddy. The patch was carried around the eddy anticyclonically and was drawn out into thin filaments. Finally it was split into two parts. To demonstrate how this kind of deformation works near the bottom of the deep sea, the deformation of a small grid due to the quasi-lagrangian transport of the points establishing the grid is shown in Fig. 10. The numbers near the grids give the simulation time in days. Again, the simulation begins on October 6 (transit of the meddy). The cyclonic rotation of the grid and its stretching after a few days is obvious. The area of the grid must remain constant, because streamfunction ψ is non-divergent. The points which leave the polygon are lost, so the simulation can only last a couple of days. In all likelihood the grids would be stretched into very thin filaments after only a few rotations. This is a condition necessary for small-scale mixing processes to work effectively and to smooth out the gradients of any inhomogeneously distributed matter or hydrographic property between the patch and the surrounding water mass; for example salinity or the concentration of nutrients.

Conclusion

The benthic storms between September '83 and September '84 obviously occur in connection with deep reaching synoptic eddies. In all probability most of the other storms in Table 1 appear also due to deep reaching vortices. Naturally not every vortex causes a benthic storm according to our definition, even though a slight increase of the near bottom velocity can always be observed. The eddies transmit a part of their kinetic energy to the BBL and the resulting increase of bottom friction enhances the height of the BBL. Such events are essential for particles which are released at the seabed or within the BBL. The pulses of high velocity flow enable the particles to cross the interface between BBL and the deep sea. Robinson and Kupferman [1985] suggested 3 mechanisms for this transfer:

1) The dismantling of the pycnocline at the top of the BBL, i. e. the reduction of the gradients of the hydrographic properties between BBL and deep sea.
2) The detatchment of parts of the BBL; or:
3) The breaking of international waves at the pycnocline.

Fig. 11 shows 3 CTD profiles with potential temperature Θ and particle concentration C. The probes are taken at nearly the same position in the central NOAMP area, but at different times, i. e. September '83, '84, and '85. The profiles A and B clearly show the sharp interface between the well-mixed BBL and the stratified interior of the deep sea. In profile C this interface is eroded. The profiles were taken by F. Nyffeler and Ch.-H. Godet, University Neuchâtel, who participated in the NOAMP cruises (Nyffeler and Godet [1986]).

Another transfer mechanism is given direct by the vortex. Matter captured by the eddy is forced to follow its movement. Synoptic eddies are known to move for several months without any significant exchange between core water and the surrounding water mass.

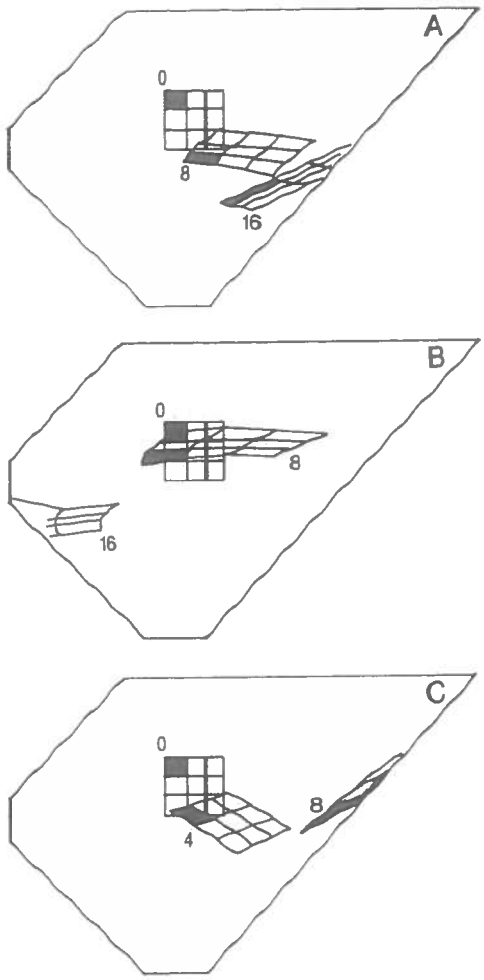

Fig. 10. Deformation of a grid at (A) 200 m, (B) 70 m, and (C) 10 m a. b. The numbers near the grid give the simulation time in days

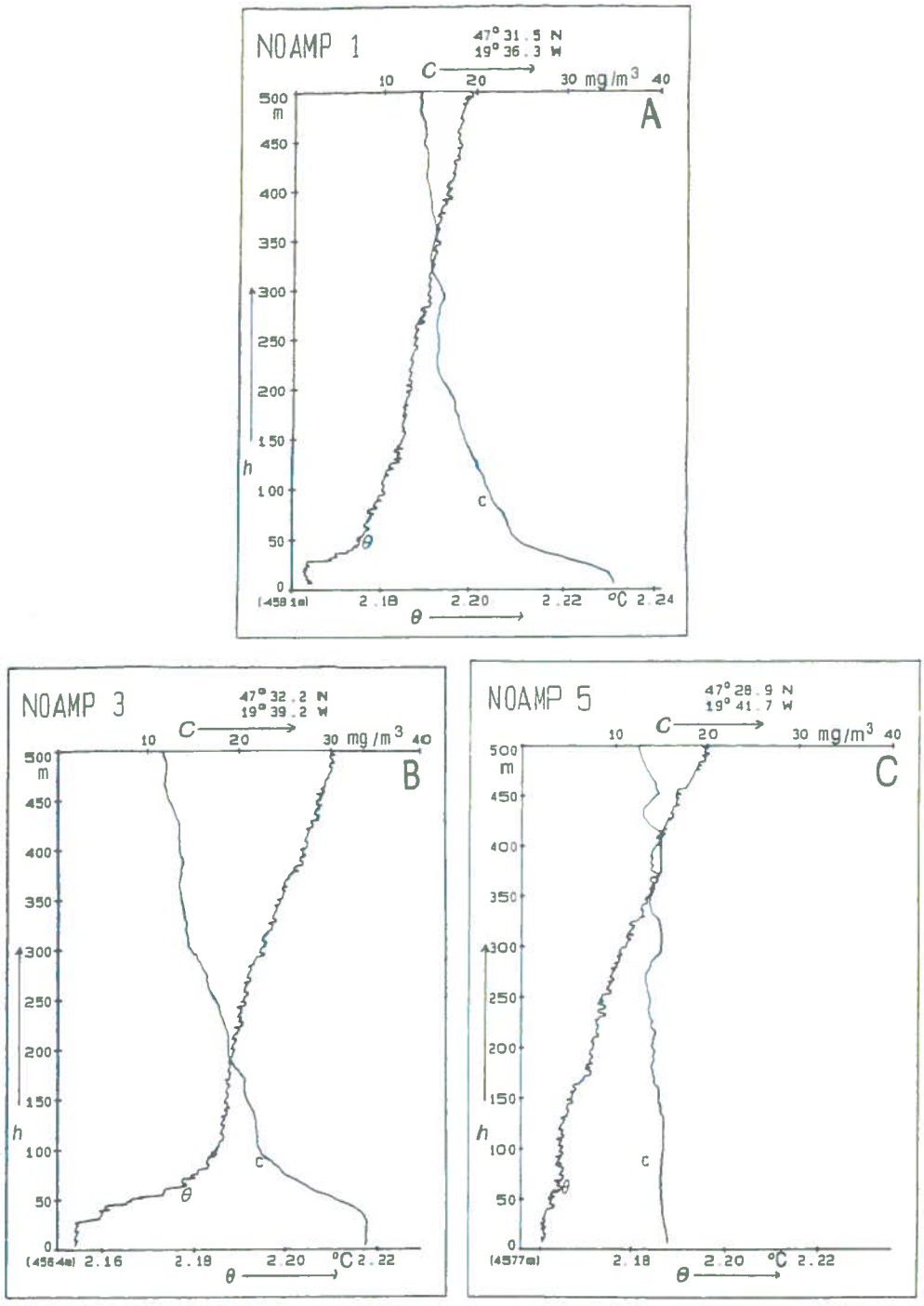

Fig. 11. CTD profiles with potential temperature Θ and particle concentration C (from Mittelstaedt et al. [1986])
The profiles are taken at the same position (±3 n. m.) but at different times (Sept. '83, '84, and '85). In (C) the gradients at the top of the BBL are eroded

If a parcel of water, which can be distinguished from the surrounding water mass, comes into contact with a vortex, shear leads to a deformation into thin filaments which can be wrapped up around the vortex. Now, small-scale mixing processes, together with the characteristic diffusivity of the tracer, flatten out the concentration to a more cloudlike distribution.

It is obvious that the necessary physical conditions for the aforementioned exchange mechanisms are present in the NOAMP area. A more detailed analyses of these processes requires better information about the vertical transport and direct measurements of lagrangian particle dispersion.

The next step will concern the data analysis of 15 deep Sofar-Floats, which were released in the NOAMP area in May '85 and have been tracked over more than one year. These data, together with CTD and current meter measurements, will enable a more quantitative analysis of dispersion and exchange processes in the deep sea.

Acknowledgements

This work was supported by the Bundesministerium für Forschung und Technologie of the Federal Republic of Germany, grants MFU 0519-9 and MFU 0556-9.

References

Armi, L., and R. C. Millard, Jr., 1976: The bottom boundary layer of the deep ocean. J. geophys. Res. **81**, 4983–4990.

Dickson, R. R., W. J. Gould, T. J. Müller, and C. Maillard, 1985: Estimates of the mean circulation in the deep (>2,000 m) layer of the Eastern North Atlantic. Progr. Oceanogr. **14**, 103–127.

Le Groupe Tourbillon, 1983: The Tourbillon Experiment: A study of a mesoscale eddy in the Eastern North Atlantic. Deep-Sea Res. **30A**, 475–511.

Heinrich, H., 1986: Bathymetrie und Geomorphologie des NOAMP Gebietes, Westeuropäisches Becken (17° W bis 22° W, 46° N bis 49° N). Dt. hydrogr. Z. **39**, 183–196.

Hollister, C. D., and I. N. McCave, 1984: Sedimentation under deep-sea storms. Nature. **309**, 220–225.

Kamenkovich, V. M., M. N. Koshlyakov and A. S. Monin, 1986: Synoptic eddies in the ocean. Dordrecht: Reidel 433 pp.

Kupferman, S. L., G. A. Becker, W. F. Simmons, U. Schauer, M. G. Marietta, and H. Nies, 1986: An intense cold core eddy in the North-East Atlantic. Nature. **319**, 474–477.

Mittelstaedt, E. (ed.), M. Bock, I. Bork, H. Klein, H. Nies, U. Schauer, 1986: Ausbreitungsbedingungen für Stoffe in großen Tiefen (NOAMP – Nordostatlantisches Monitoring-Programm). Hamburg: Deutsches Hydrogr. Institut. 202 S. m. Abb. u. Tab.

Mittelstaedt, E. 1987: Cyclonic cold-core eddy in the Eastern North Atlantic. I. Physical description. Mar. Ecol. Progr. Ser. **39**, 145–152.

Nyffeler, F. and Ch.-H. Godet, 1986: The structural parameters of the benthic nepheloid layer in the northeast Atlantic. Deep-Sea Res. **33**, 195–207.

Robinson, A. R., and S. L. Kupferman, 1985: Dispersal from deep ocean sources: Physical related scientific processes. Sandia-Report. SAND82–1986.

Schauer, U., 1987: A deep cyclonic meddy in the West European Basin. Internat. Council for the Exploration of the sea. C. M. 1987/C:27.

Streeter, V. L. (ed.), 1961: Handbook of fluid dynamics. New York [usw.]: McGraw-Hill.

Vangriesheim, A., 1986: Dynamique et hydrologie de la couche profonde dans l'Atlantique Nord-Est. Campagnes Oceanographiques Francaises. No. 2. IFREMER, Centre de Brest.

Eingegangen am 2. September 1987

Angenommen am 23. September 1987

Anschrift des Verfassers:
Holger Klein, Deutsches Hydrographisches Institut, Bernhard-Nocht-Straße 78, 2000 Hamburg 4